Advances in Radiation Oncology (2021) 7, 100867

advances in radiation oncology

www.advancesradonc.org

Scientific Article

Development of an Orthotopic Murine Model of Rectal Cancer in Conjunction With Targeted Short-Course Radiation Therapy

Taylor P. Uccello, MS,[a] Sarah A. Kintzel, BS,[b] Bradley N. Mills, PhD,[c] Joseph D. Murphy, MS,[a] Jesse Garrett-Larsen, BS,[c] Nicholas G. Battaglia, PhD,[a] Carlos J. Rodriguez, BS,[a] Michael G. Drage, MD,[d] Jian Ye, PhD,[c] Tanzy M.T. Love, PhD,[e] Carl J. Johnston, PhD,[f] Elizabeth A. Repasky, PhD,[g] Haoming Qiu, MD,[h] David C. Linehan, MD,[c] Edith M. Lord, PhD,[a] and Scott A. Gerber, PhD[a,c,*]

[a]Department of Microbiology and Immunology, University of Rochester Medical Center, Rochester, New York; [b]Department of Biomedical Engineering, University of Rochester Medical Center, Rochester, New York; [c]Department of Surgery, University of Rochester Medical Center, Rochester, New York; [d]Department of Pathology and Laboratory Medicine, University of Rochester Medical Center, Rochester, New York; [e]Department of Biostatistics and Computational Biology, University of Rochester, Rochester, New York; [f]Department of Pediatrics, University of Rochester Medical Center, Rochester, New York; [g]Roswell Park Comprehensive Cancer Center, University at Buffalo, Buffalo, New York; [h]Department of Radiation Oncology, University of Rochester Medical Center, Rochester, New York

Received September 2, 2021; accepted November 16, 2021

Abstract

Purpose: Orthotopic tumors more closely recapitulate human cancers than do ectopic models; however, precision targeting of such internal tumors for radiation therapy (RT) without inducing systemic toxicity remains a barrier. We developed an innovative murine orthotopic rectal tumor model where the insertion of clinical grade titanium fiducial clips on opposing sides of the rectal tumor allowed for targeted administration of short-course radiation therapy (SCRT). With this novel approach, clinically relevant RT regimens can be administered to orthotopic tumors to explore the biology and efficacy of radiation alone or as a combination therapy in a murine model that closely recapitulates human disease.

Methods and Materials: Murine Colon 38-luciferase tumor cells were injected into the rectal wall of syngeneic mice, and fiducial clips were applied to demarcate the tumor. An SCRT regimen consisting of 5 consecutive daily doses of 5 Gy delivered by an image-guided conformal small animal irradiator was administered 9 days after implantation. Tumor burden and survival were monitored along with histological and flow cytometric analyses on irradiated versus untreated tumors at various time points.

Results: SCRT administered to orthotopic rectal tumors resulted in a reduction in tumor burden and enhanced overall survival with no apparent signs of systemic toxicity. This treatment paradigm resulted in significant reductions in tumor cellularity and increases in fibrosis and hyaluronic acid production, recapitulating the SCRT-induced effects observed in human cancers.

Sources of support: This work was supported by grants R01CA236390 (S.G., E.R.) and R01CA230277 (S.G.) from the National Cancer Institute, and grant AI007285 (T. U.) from the National Institutes of Health.

Disclosures: none.

Research data are stored in an institutional repository and will be shared upon request to the corresponding author.

*Corresponding author: Scott A. Gerber, PhD; E-mail: Scott_Gerber@urmc.rochester.edu

https://doi.org/10.1016/j.adro.2021.100867

Conclusions: We have established a means to target murine orthotopic rectal tumors using fiducial markers with a fractionated and clinically relevant SCRT schedule that results in an RT response similar to what is observed in human rectal cancer. We also validated our model through examining various parameters associated with human cancer that are influenced by irradiation. This model can be used to further explore RT doses and scheduling, and to test combinatorial therapies.

Introduction

Rectal cancer (RC) is the second leading cause of cancer-related deaths worldwide.[1] Total mesorectal excision surgery is a common treatment approach, but remains limited by significant morbidity and can negatively impact quality of life.[2] Preoperative radiation therapy (RT) is often administered to avoid surgery and retain tissue function;[3−6] however, only a fraction of patients will demonstrate complete clinical responses following RT (approximately 20%), while the majority will require invasive excision surgery. The factors mediating interpatient responses to preoperative RT remain largely unknown.

Established preclinical mouse models that accurately recapitulate human disease are paramount for investigation of the rectal RT response phenomena in order to improve the clinical response rate. Currently, the majority of rectal tumor models involve subcutaneous or intramuscular injection of tumor cells (ie, ectopic models). Although such models are highly reproducible, noninvasive, and simple, they do not recapitulate the microenvironment of most human diseases, and, consequently, many therapeutics that are successful in murine models fail in human trials.[7] Orthotopic tumor models overcome the aforementioned limitations of the ectopic model; however, targeting these internal tumors with clinically relevant RT while avoiding gut toxicity is a major barrier. As far as we are aware, no published model employs clinically relevant RT directly to the orthotopic tumor. A recent review by Gillespie et al highlighted this unmet need and acknowledged that newly available research platforms capable of delivering clinically relevant image-guided RT to anatomically accurate tumors will allow for compulsory studies exploring the efficacy of RT in RC.[8] Here we describe a method that utilizes fiducial markers and computed tomography (CT) imaging to demarcate tumor margins, allowing for precision targeting of RT to internal orthotopic rectal tumors.

We developed an innovative mouse model where Murine Colon 38 (MC38) adenocarcinoma tumor cells are injected into the rectal wall of syngeneic C57BL/6 mice, and clinically relevant titanium fiducial clips are surgically inserted on opposing sides of the tumor to help delineate tumor margins via CT. The rectal tumors were treated with a fractionated schedule of 5 consecutive daily doses of 5 Gy per dose using image-guided conformal small animal irradiator technology, as modeled after the standard-of-care for RC patients, known as short-course radiation therapy (SCRT).[4,9] Using this approach, we demonstrated that SCRT was effective in prolonging survival with minimal toxicity to normal tissue, which is similar to outcomes observed clinically. Tumor microenvironmental parameters known to influence both the efficacy and outcome of RT were also assessed for further validation. Hypoxia, a key hallmark in most human cancers that has a negative impact on RT, was identified as early as 4 days post-tumor implantation and remained constant as the tumor progressed. The hypofractionation schedule reduced tumor hypoxia, likely a result of RT-induced reoxygenation.[10] Fibrosis is a chronic complication associated with RT[11] and was detected shortly following the completion of SCRT as both collagen and hyaluronic acid (HA) were elevated in the extracellular matrix (ECM). Accordingly, our model not only recapitulates human RC disease, but also describes a clinically relevant technique to assess the efficacy and outcome of SCRT in orthotopic rectal tumors.

Materials and Methods

In vivo animal studies

All experiments were approved by the University Committee on Animal Resources and were performed in compliance with both National Institutes of Health and University-approved guidelines for the care and use of animals. Six- to 8-week-old age-matched female C57BL/6J mice (Jackson Laboratory) were used. All mice were subjected to a 12-hour light/dark cycle and kept in individually ventilated cages with bedding and nesting material.

Cell culture

MC38-parental cells syngeneic to the C57BL/6 background were obtained from ATCC (Manassas, Virginia). MC38-parental cells were stably transfected with the firefly luciferase plasmid, and bulk luciferase positive cells were obtained and clones selected (MC38-luc). MC38-luc were cultured in MAT/P (US patent No. 4.816.401) supplemented with 2% fetal bovine serum (GIBCO), and 1% penicillin/streptomycin (Thermo Fisher Scientific) in T75 flasks and incubated at 37°C, 5% CO_2.

Evans blue toxicity assay

MC38-luc cells were plated at 3×10^5 cells/well in a 6-well dish. Once adhered, varying concentrations of Evans

blue dye (Sigma Aldrich) were introduced to the culture (0%, 0.0625%. 0.03125%, 0.015625%, and 0.0078125%). Cells were collected every 10 minutes for 50 minutes total and counted using trypan blue stain (Invitrogen). The number of live and dead cells were calculated for each condition at each time point.

Orthotopic tumor mouse model

Six- to 8-week-old female, C57BL/6 mice were injected subcutaneously with SR buprenorphine (Ethiqua) prior to surgery to minimize pain. MC38-luc cells were prepared at 2.5×10^4 cells/5 μL of a 1:1 ratio of Evans blue to Matrigel matrix (BD Bioscience). Mice were anesthetized using isoflurane (Vet One Fluoriso) and shaved in the abdominal region. Prior to incision, feces were expelled by gently palpating the lower abdomen of anesthetized mice to clear the intestinal tract and aid in an accurate injection. The surgical area was sanitized with iodine, a small incision was made in the lower abdomen, and the rectum was gently retracted by forceps. The rectum was exposed and 5 μL of cells were injected into the rectal wall using a 32-gauge Hamilton syringe. Pausing for 5 seconds after tumor injection prior to removing the needle prevented cell leakage into the peritoneal cavity. The peritoneal wall was sutured, and the skin was stapled together. Mice were returned to a cage with a water-jacketed heating source for 1 hour until recovered from anesthetic and monitored for 3 days. For radiation studies, 8 days following initial tumor injection, mice were again anesthetized using isoflurane and reopened. Titanium fiducial clips were implanted directly on either side of the tumor tissue and the mice were closed as described prior. Again, mice were monitored for 3 days.

Monitoring tumor burden by bioluminescence

Tumor-bearing anesthetized mice were injected with a luciferin substrate (2.5 mg/100 μL phosphate-buffered saline [PBS], Invitrogen) subcutaneously that emits light when cleaved by luciferase-expressing tumor cells. This bioluminescent light is detected by an in vivo imaging system (IVIS) where the number of photons per second within an area of interest corresponds with tumor burden. Mice were placed in a supine position and 12 consecutive images were taken at 2-minute intervals. Regions of interest were drawn around the tumor region and the maximum bioluminescence (BLI) reading over the course of the 12 images was recorded.

Histology

Following sacrifice, tumor and metastasis were excised and fixed in 10% neutral buffered formalin (Azer Scientific). Samples were paraffin embedded, sectioned into 5 micron slices, and stained with hematoxylin (VWR) and eosin with phylocine (Richard Allan Scientific, Thermo Fisher Scientific), trichome (New Comer), or hyaluronic acid binding protein (Millipore Sigma). Histology was quantified by algorithms generated using ImageScope Software (Aperio).

Whole mount immunofluorescence

Mice were sacrificed and small tumor pieces (MC38-GFP; $\sim 2 \times 3 \times 1$ mm) were excised. Samples were placed in 6 mL polypropylene tubes and blocked using Fc Block (PharMingen, San Diego, CA) at 10 μg/mL in 200 μL of PAB (phosphate-buffered saline, 0.1% sodium azide, 1% bovine serum albumin; Sigma Aldrich) for 15 minutes at 4°C. Antibodies (CD31-APC) were added directly to tubes and incubated for 2 hours at 4°C. Samples were washed twice by the addition of 4 mL PAB and rotated at 4°C for 30 minutes. After the final wash, samples were collected from the tubes and placed on glass slides with PAB. A coverslip was placed on top of the tumor and pressed down. Samples were viewed via fluorescence microscopy and digital images were acquired. Pseudo color was added to the digital images using ImageJ (Fuji).

Flow cytometry

Tumor-bearing mice were sacrificed, and tumors were extracted, weighed, and homogenized manually in collagenase (Sigma Aldrich) and diluted in Hanks balanced salt solution (Sigma Aldrich). Partly homogenized tumors were processed further using gentle Macs homogenizer (Miltenyl Biotec). Homogenized tumors were filtered using a 70 micron filter and then resuspended in PAB. One million cells per sample were stained for various surface markers using appropriate antibodies for 45 minutes at 4°C in the dark. Samples were washed and then resuspended in Cyto-Perm/CytoFix (BD Bioscience) for 20 minutes at 4°C in the dark, followed by a wash step in PAB. Fifty thousand events were collected on an LSRII (BD Biosciences) and results were analyzed using FlowJo software.

Hypoxia staining

Mice were injected retro-orbitally with 150 μg EF5 (EMD Millipore Sigma) or PBS 3 hours prior to sacrifice. Mice were euthanized by cervical dislocation and tumors were extracted.

For immunofluorescence: Tumors were immediately excised and embedded in OCT (Sakura Tissue Tek) and frozen. Samples were cut using a microtome (Leica CM1950) into 10 micron sections. Slides were fixed in paraformaldehyde for 1 hour at room temperature. Following fixation, slides were washed twice for 10 minutes

per wash with PBS and then blocked overnight at 2°C to 8°C with blocking solution (10% nonfat dry milk, 0.4 mL mouse IgG, 0.12 g lipid-free albumin, and 6 mL 1xttPBS [100% Tween, sodium azide, sterile PBS]). The following day, blocking buffer was removed and slides were rinsed in 1xttPBS. Next, ELK-Cy3 (EMD Millipore Sigma) was added to each slide, along with CD31-BV480 and incubated at 4°C for 1 hour. Slides were then washed twice with ttPBS (45 minutes), followed by 45 minutes with PBS. Cover slides were applied, and slides were imaged using fluorescent microscopy.

For flow cytometry: Tumors were processed as explained prior. Following traditional intracellular staining, cells were fixed in 4% paraformaldehyde for 1 hour at 4°C. Cells were rinsed 3 times with PBS and resuspended in blocking solution overnight at 4°C. The following day, blocking buffer was removed and cells were rinsed in 1xttPBS. Cells were then stained in ELK Cy3 (75 μg/mL) in antibody dilution buffer (100 mL 1xttPBS, 1.5 g lipid-free albumin) for 3 hours at 4°C. Cells were then rinsed 3 times for 1 hour (ttPBS for the first 2 washes, then in PBS). Cells were finally resuspended in 1% paraformaldehyde and events were collected on LSRII.

Radiation therapy

Mice were anesthetized with isoflurane and then irradiated using the small animal research radiation platform (SARRP; XStrahl, Augusta, GA). The SARRP incorporates cone-beam computed tomography (CBCT) imaging with precise radiation delivery to pinpoint an exact anatomical target and deliver 0.5 mm beams to that point. Mice are anesthetized and a CBCT image consisting of 1440 projections is acquired to identify the tumor/fiducial markers. The data are transferred to radiation planning software, Muriplan (Xstrahl), where the CBCT image is registered, and simple segmentation of tissues is performed separating air, lung, fat, tissue, and bone. An isocenter is positioned within the tumor and the intended dose is prescribed to the isocenter. In this application, 2 opposing beams delivered through a 5 × 5 mm collimator (5 Gy/tumor/day for 5 days) were delivered from day 9 through day 13 at beam angles of -91 and 89 degrees, which reduce radiation exposure to the areas of backbone, stomach, small intestine, and spleen. Beam energy of 220 kVp with a 0.15 mm Cu filter, 0.6 mm Cu HVL tube current, and 12 mA beam current dose rate were utilized. Contouring and isodose lines are provided and monitored to ensure intended radiation dose was delivered consistently throughout the tumor.

Statistical analysis

Statistical analysis was performed using Prism 8 software (GraphPad). Data are presented as mean ± standard deviation. Significance was determined by unpaired nonparametric Mann-Whitney *t* test. For multiple group comparisons, significance was determined by ordinary one-way analysis of variance with multiple comparison post hoc tests. Bioluminescent growth curves plotted as geometric mean with standard deviation. Survival was determined by the Mantel-Cox test ($P < .05$).

Results

Establishment of an orthotopic injection into the rectal submucosa and in vivo imaging of tumor burden

The most common form of human RC is adenocarcinoma,[12] which commonly invades the submucosal layer of the rectal wall.[13] Accordingly, we developed an orthotopic murine model of RC that manifests in a similar location to human disease. Tumor cells were resuspended in a 1:1 mixture of Evans blue dye and Matrigel matrix, a liquid that hardens at body temperature providing essential growth factors and a scaffold for the injected cells. Evans blue allowed for the visualization and tracking of rectal wall injections, and toxicity was assessed by monitoring cell viability in vitro using various concentrations of dye. A concentration of 7.8×10^{-3}% was found to have minimal effect on cell viability, but was dark enough for visualization (Fig E1a). A surgical incision was made in the lower abdomen and the rectum was gently retracted by forceps. Tumor cells were injected in the rectal wall using a 32-gauge Hamilton syringe (Fig 1A). Pausing for 5 seconds after tumor injection prior to removing the needle prevented cell leakage into the peritoneal cavity. We determined that the rectal wall can hold a maximum of 5 μL of injected fluid, as larger volumes resulted in unavoidable leakage and subsequent peritoneal deposits (data not shown). Importantly, physiologically relevant tumors do not impede the ability to defecate.

MC38 cells are a well-established tumor line that is syngeneic to the C57BL/6 mouse and is used extensively to model colorectal cancer.[14] To enable noninvasive, longitudinal monitoring of tumor growth in vivo, we stably transfected the MC38 tumor cell line with a plasmid containing the firefly luciferase gene and selected a luciferase-expressing clone that grows at a similar rate to parental cells (data not shown). BLI in the lower abdominal region was detected using the IVIS Imaging System (PerkinElmer) as early as 6 days following tumor inoculation (Fig E2a). Orthotopic tumors successfully seeded in 100% of mice, and progressed consistently (Fig E2b) until mice succumbed to disease, with a mean overall survival of 30 days (Fig E2c).

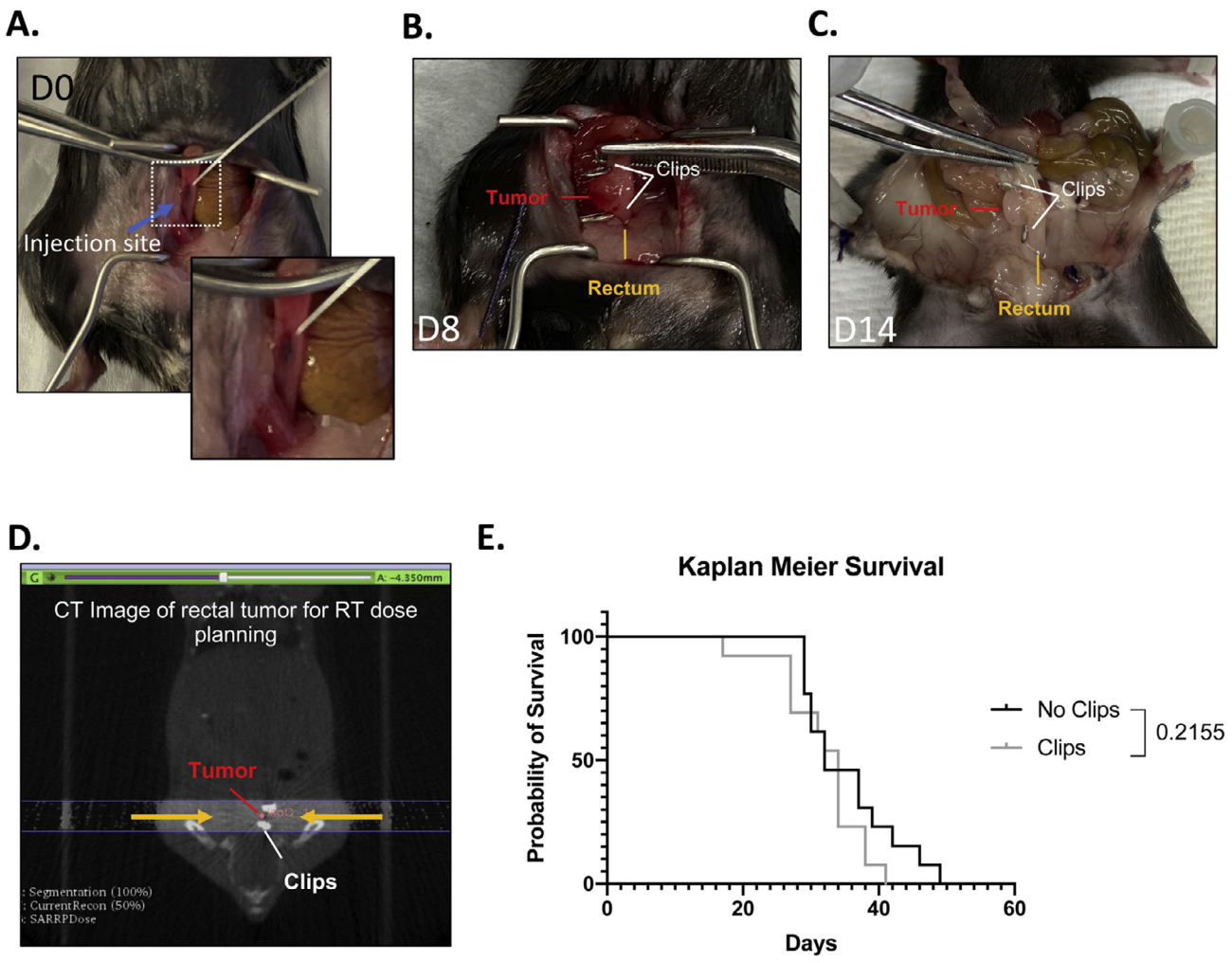

Figure 1 Evidence of a clinically relevant model. **(A)** 2.5×10^4 MC38-luc cells in 5 μL of a 1:1 Matrigel/Evans blue solution (7.8×10^{-3}%) were injected into the rectal membrane wall using a Hamilton syringe (blue arrow). **(B)** Fiducial clips implanted on day 8 on opposing sides of tumor. **(C)** After the full course of short-course radiation therapy, fiducial clips remain on opposing sides of growing tumor. **(D)** Fiducial clips visible by computed tomography enable precise targeting of the tumor using the small animal research radiation platform. **(E)** Incorporation of fiducial clips has no effect on mouse survival. Significance determined by log rank Mantel-Cox test. *Abbreviations:* CT = computed tomography; D = day; RT = radiation therapy.

Development of a clinically relevant technique to identify tumors by CT imaging

Fiducial markers are commonly used in radiation oncology to identify internal tumors.[15] We established a clinically relevant strategy for identifying RC tumors by implanting titanium fiducial clips on opposing sides of the actual rectal tumor 8 days following initial injection (Fig 1B). Clip location shifted with coordinate tumor growth, but still accurately delineated tumor margins throughout the course of radiation (Fig 1C). Clips were identified by CT imaging and the isocenter of radiation was administered directly between the 2 markers using the SARRP (Fig 1D). Importantly, clip placement and the additional surgery did not affect overall survival of these animals (Fig 1E).

Radiation reduces tumor burden and enhances survival while avoiding off-target and systemic toxicity

Tumors were treated with the SARRP using 2 opposing beam angles of high energy x-rays to the tumor, and treatment targeting plans were individualized for each animal. The RT schedule and dose mirrored clinical SCRT and consisted of 5 consecutive daily doses of 5 Gy per dose from day 9 through day 13 postimplantation (Fig 2A).

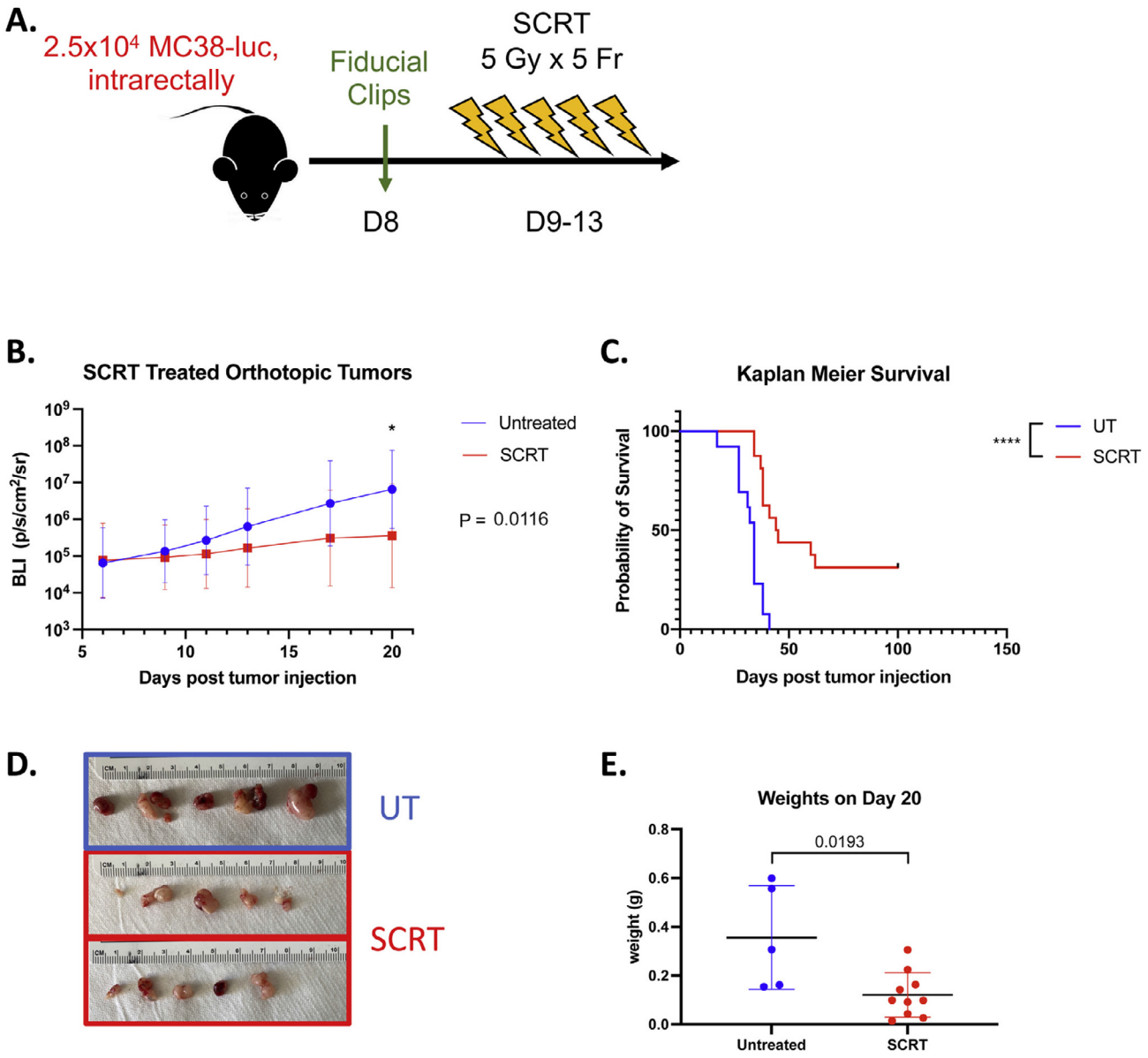

Figure 2 SCRT results in a reduction of tumor burden and significant increase in overall survival. **(A)** 2.5×10^4 MC38-luc cells were injected orthotopically on day 0, fiducial clips implanted on day 8, and SCRT (5 Gy per fraction for 5 consecutive fractions) was administered on days 9 to 13. **(B)** Bioluminescent growth curve following SCRT (red) compared to UT (blue); data are plotted as geometrical mean with standard deviation. Significance determined by unpaired *t* test. **(C)** Kaplan-Meier survival curve demonstrating significantly enhanced overall survival in irradiated mice. Significance determined by log-rank Mantel-Cox test. **(D)** Tumor sizes and **(E)** weights on day 20 following SCRT. Significance determined by unpaired *t* test. *Abbreviations:* D = day; SCRT = short-course radiation therapy; UT = untreated.

Mice that received SCRT demonstrated a significant reduction in tumor burden (Fig 2B) and enhanced overall survival out to 100 days postinjection (Fig 2C) compared with untreated controls. Tumor size (Fig 2D) and weight (Fig 2E) measurements performed on day 20 corroborated BLI findings, indicating that irradiated tumors were significantly smaller than untreated tumors.

Normal tissue damage is a potential side effect of treating RC with RT. Off-target toxicity was determined to be negligible based on dose volume histograms of adjacent tissue (Fig 3A, Fig 3B). This confirmed full dose deposition to the tumor and insignificant amounts to nearby tissue, namely the abdominal cavity and spinal column. Additionally, mouse weight was monitored starting 6 days prior to SCRT. Although animal weights declined initially following surgery (day 8), losses stabilized, and there were no significant differences between the untreated and irradiated groups, indicating a lack of RT-induced toxicity (Fig 3C).

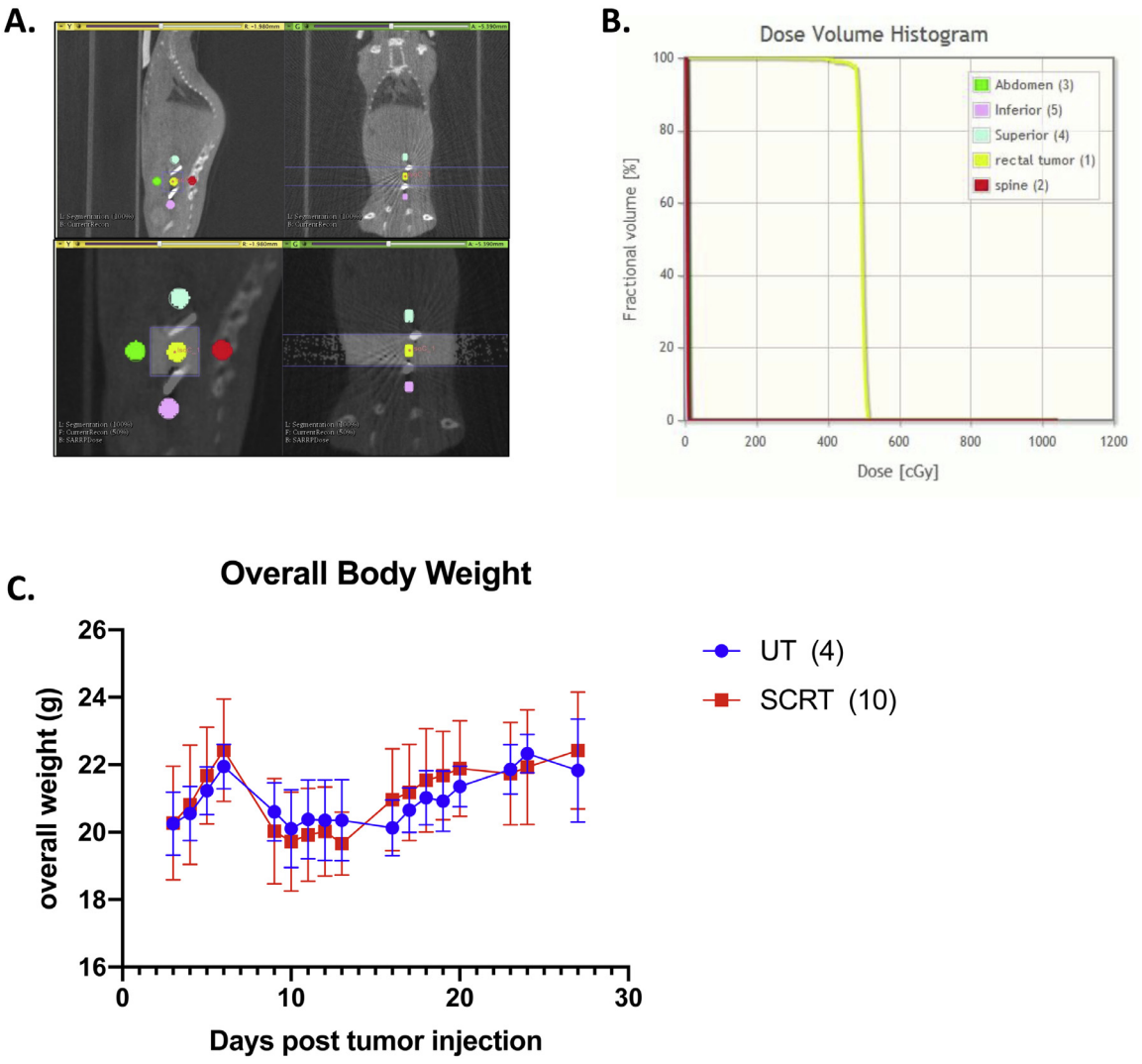

Figure 3 No toxicity was associated with SCRT. **(A, B)** Dose volume histogram calculated from SCRT regimen for tumor and adjacent normal tissue. **(C)** Overall body weight of irradiated (SCRT; red) or untreated (UT; blue) animals starting on day 3 and followed up to 27 days post−tumor injection; numbers in parentheses indicate number of mice. *Abbreviations:* SCRT = short-course radiation therapy; UT = untreated.

Reduced tumor cellularity following SCRT

Preoperative RT is essential in debulking tumors in order to facilitate surgical resection.[16] We hypothesized that SCRT would reduce the cellular density of treated tumors. Hematoxylin and eosin (H&E) staining of day 14 RC tumors annotated by a board-certified pathologist revealed a monotonous, cohesive, spindle cell population with tissue-destructive, expansile growth and well-circumscribed borders, involving colon and adjacent soft tissue. As the tumors increased in size, by day 14 areas of hypocellularity and frank tumor necrosis became apparent, likely reflecting growth beyond vascular support (data not shown). The H&E stains were further analyzed using ImageScope to measure positive nuclei staining (Fig 4A, Fig 4B), and results demonstrated that RT acutely reduced cell density. We observed similar cellularity levels 5 days following the final fraction of SCRT (day 18), demonstrating a sustained response (Fig 4C). This reduction largely resulted from decreases in the number of CD45- cells, as CD45+ immune populations remained constant as determined by flow cytometry (Fig 4D, Fig 4E).

Rectal tumors establish vasculature and intratumoral hypoxia

Tumors require prominent vasculature formation to support enhanced growth via a process known as angiogenesis. We utilized whole mount fluorescence microscopy to monitor the angiogenic switch, a key event that marks the initiation of neovasculature. MC38-GFP (green fluorescent protein) orthotopic tumors were harvested at various

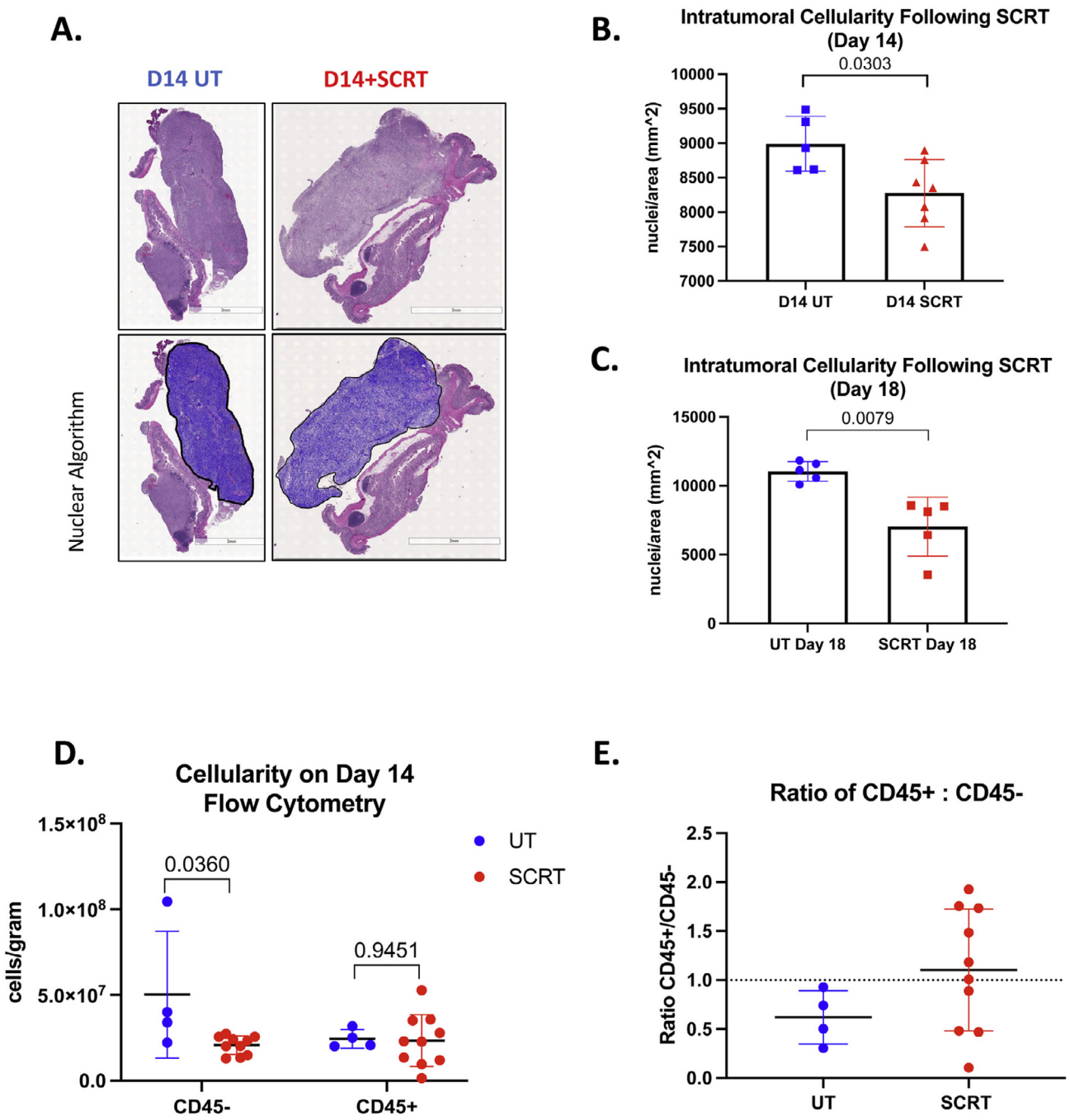

Figure 4 Cellularity following SCRT. **(A)** Representative H&E images of untreated (UT; left) and irradiated (SCRT; right) tumors on day 14. Tumor margins annotated (bottom; black outline). Positive nuclei in the tumor were determined using an algorithm in ImageScope software (bottom). **(B, C)** Quantification of nuclei per area of tumor on days 14 and 18. Significance determined by unpaired *t* test. **(D)** Flow cytometry performed on day 14 rectal tumors. Significance determined by unpaired *t* test. **(E)** Ratio of immune (CD45+) to nonimmune (CD45-) cells in the rectal tumors. *Abbreviations:* D = day; H&E = hematoxylin and eosin; SCRT = short-course radiation therapy; UT = untreated.

time points to monitor the establishment of new blood vessels by co-staining with fluorescently labeled anti-CD31. The tumor boundary was clearly identified at day 6 (Fig 5A) as the interface of the tumor with normal rectum depicted tortuous vessels inside the tumor boundary, with organized vasculature in the adjacent normal rectum (Fig 5B). Disorganized neovasculature was observed as early as day 4 within the tumor (Fig 5C), along with the

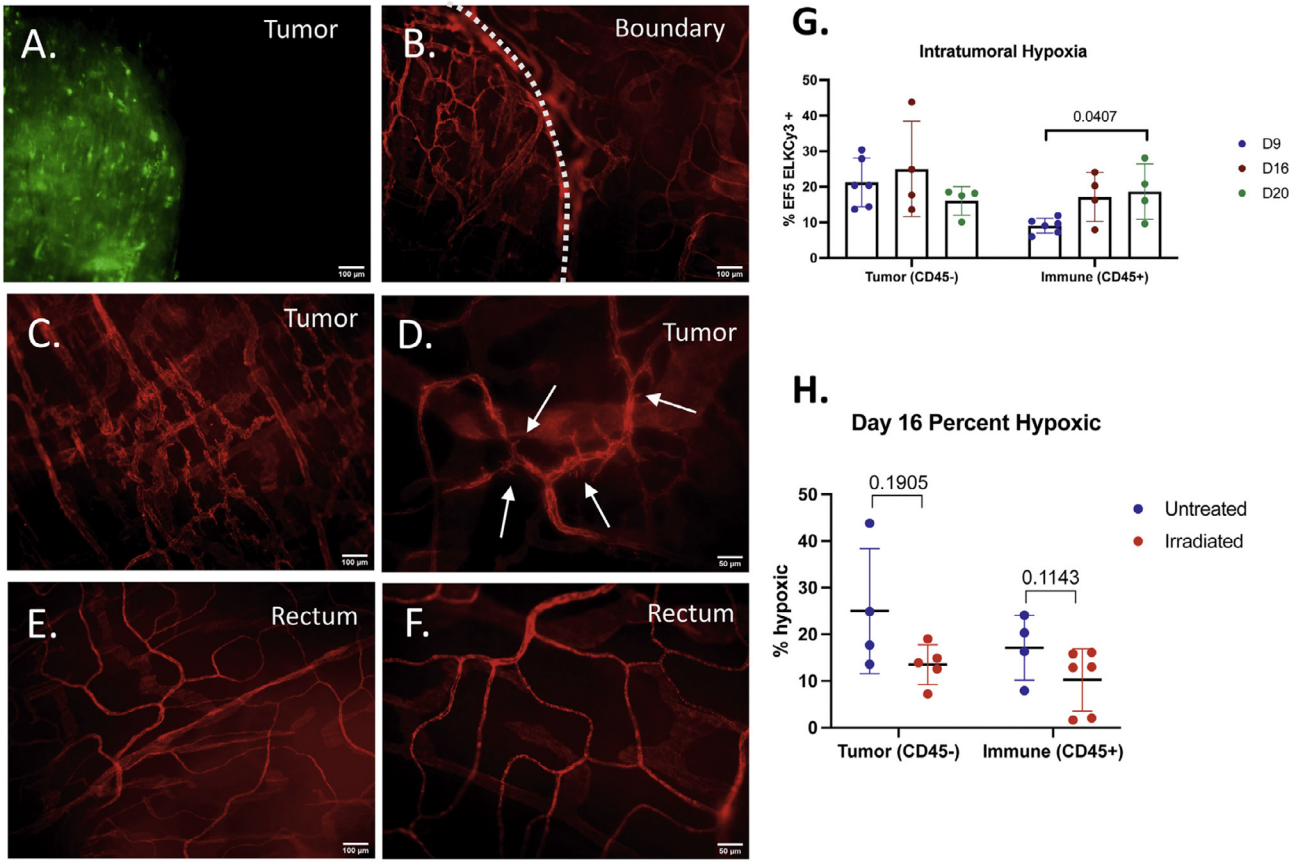

Figure 5 Establishment of vasculature and hypoxia within the rectal tumors. Day 4 and day 6 wholemount of MC38-GFP orthotopic tumors stained with anti-CD31 (blood vessels). **(A)** 10 × day 6 MC38-GFP tumor. **(B)** 10 × day 6 tumor boundary. Anti-CD31 co-stained with gray dashed line indicating tumor boundary. **(C)** 10 × anti-CD31 day 4 tumor. **(D)** 20 × anti-CD31 day 4 tumor with white arrows indicating angiogenic sprouts. **(E)** 10 × anti-CD31 day 4 normal rectal tissue. **(F)** 20 × anti-CD31 day 4 normal rectal tissue. **(G)** Percentage of intratumoral hypoxic tumor cells (CD45-) and immune cells (CD45+) from untreated rectal tumors on day 9, 16, 20. Significance determined by ordinary one-way analysis of variance. **(H)** Percent of hypoxic tumor (CD45-) and immune cells (CD45+) on day 16 following SCRT. Significance determined by unpaired *t* test. *Abbreviation:* D = day; SCRT = short-course radiation therapy.

formation of angiogenic sprouts (Fig 5D, white arrows). Comparatively, vasculature in the normal adjacent rectum appeared to be orderly at this time point (Fig 5E, Fig 5F).

Hypoxia is a major hallmark of solid tumors despite the presence of abundant vasculature throughout the tumor microenvironment (TME), and is observed clinically in RC.[17] Additionally, hypoxia is a negative indicator of overall survival for RC patients.[17] We investigated whether our preclinical orthotopic model recapitulated this key aspect of human cancer. Areas of hypoxia were visualized by immunofluorescence and quantified by flow cytometry as described in the materials and methods. Regions of intratumoral hypoxia were observed throughout the tumor on day 24 (representative image, Fig E3). Using flow cytometry, we determined that approximately 20% of the viable tumor cells (CD45-negative population) were hypoxic as early as day 9 and this level persisted as tumors matured (Fig 5G, left). In contrast, significant increases in the hypoxic fraction of intratumoral immune populations (CD45+) were observed over time (Fig 5G, right). A hypofractionated RT schedule often results in a reoxygenation phenomenon that enhances the efficacy of therapy.[10] We examined whether SCRT reduced intratumoral hypoxia in our model. Although the values did not reach significance, we did observe trending decreases in the percent of both hypoxic tumor cells (CD45-) and tumor-infiltrating immune cells (CD45+) from tumors harvested on day 16 (Fig 5H).

Changes in the ECM following SCRT

Fibrosis is an important component of the TME, and its dysregulation during tumor growth can elicit both pro- and anti-tumor effects, depending on the stage of

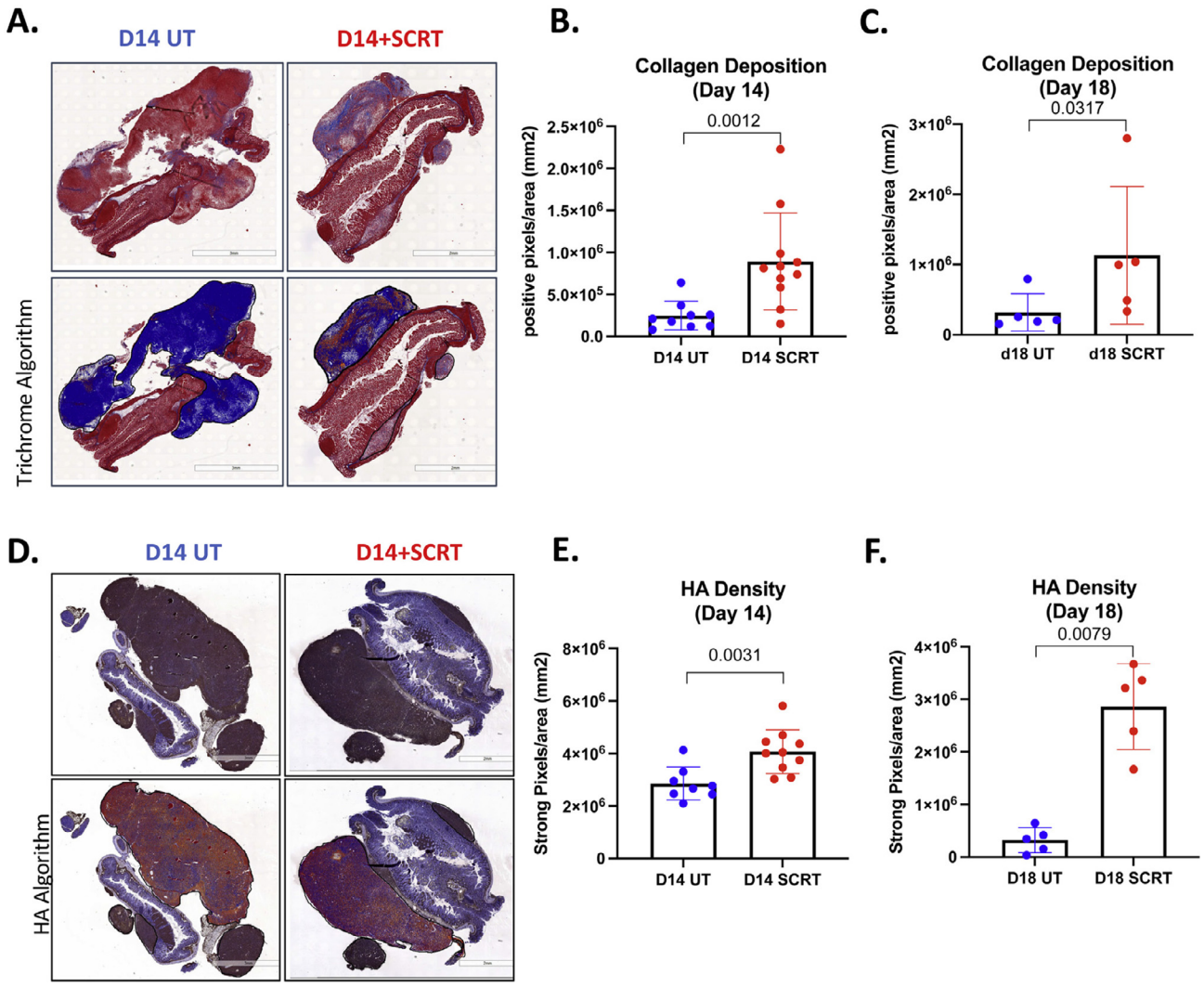

Figure 6 ECM changes following SCRT. **(A)** Representative images of untreated (UT; left) and irradiated (SCRT; right) tumors on day 14 with trichrome stain. Tumor margins annotated (bottom; black outline). Collagen pixels in the tumor were determined using an algorithm in ImageScope software (bottom). **(B, C)** Quantification of fibrosis per area of tumor on days 14 and 18. Significance determined by unpaired *t* test. **(D)** Representative images of HA stain on day 14 with positive HA pixels determined by ImageScope. Significance determined by unpaired *t* test. **(E, F).** Quantification of HA on days 14 and 18. Significance determined by unpaired *t* test. *Abbreviations:* D = day; ECM = extracellular matrix; HA = hyaluronic acid; SCRT = short course radiation therapy; UT = untreated.

tumor progression.[18] RT activates fibroblasts to produce additional ECM.[19,20] Accordingly, we investigated how SCRT modulated these factors in our orthotopic model by first measuring collagen deposition within the tumor (Fig 6A). Image analysis demonstrated that irradiated samples had significantly increased collagen levels within the tumor compared to the unirradiated controls on both days 14 and 18 (Fig 6B, Fig 6C). HA is an RT-induced ECM component of RC that is associated with poor prognosis due to observed radioprotection and anti-apoptotic signaling effects.[21] We assessed whether radiation influenced the concentration of HA in our model. Histological analysis of samples stained for HA binding protein and quantified using Aperio software demonstrated an increase of HA following SCRT on days 14 and 18 (Fig 6D-F).

Overall, our model recapitulates many key features observed clinically in RC therapy including SCRT-induced increases in both collagen and HA. These data further validate this model as a viable technique to investigate RT responses in this specific malignancy.

Discussion

Here we describe the development of an orthotopic model of RC that incorporates an innovative methodology to locate and treat tumors with RT. This was

accomplished by the placement of fiducial clips that permit targeting of the internal tumors with an SCRT dose akin to what is used in the clinic. Approximately 30% of the irradiated tumors (5 of 16 mice) show no sign of tumor burden at sacrifice (100 days), and off-target toxicity is negligible, with no observation of any systemic damage. Accordingly, the model presented here is feasible, reproducible, and, importantly, clinically relevant.

We have determined that our RT targeting scheme is highly reproducible as we consistently see a reduction in tumor burden in irradiated mice (77% decrease in BLI on day 20). Additionally, on assessment of the TME and certain parameters often associated with the RT response, our findings were similar to what is expected in the clinic. For example, we observe a significant reduction in tumor cell density at 2 separate time points. This is to be expected since SCRT would target highly proliferative tumor cells. We did not detect changes in the CD45+ immune cell population as a whole in this model. Specific immune populations such as macrophages, which typically constitute a large proportion of the intratumoral immune cells, are largely radioresistant and may be unaffected by SCRT. Additionally, RT is known to promote inflammation, including cytokines and chemotactic factors that attract immune cells to the irradiated tumor.[22] This influx of "new" immune cells into the TME may compensate for the RT-induced loss of radiosensitive immune populations, such as lymphocytes. In addition, well characterized signs of RT-induced fibrosis frequently seen in human disease replenishing areas of reduced tumor cellularity following RT treatment are observed in our model. This is particularly important since post-RT fibrosis is a common complication and consequence of treatment for RC.[11] We see consistently increased levels of fibrosis following SCRT in our model.

Valuable insight was gained while optimizing this model. The number of tumor cells injected as well as the timing of SCRT treatment were both comprehensively trialed. Initially, fewer tumor cells were injected, but resulted in a take rate of only 75%. This would make it difficult to determine which tumors responded to SCRT versus those that spontaneously rejected. Once a 100% take rate was observed, we then optimized the SCRT timing. We initially irradiated tumors at an earlier time point (days 7 through 11); however, the tumors were too small to accurately demarcate with fiducial clips and precision targeting was lost. Later time points (days 11 through 15) were also investigated; however, the tumors were quite large at the start of SCRT and would not fit entirely in the field of radiation using a 5 × 5 mm collimator. A larger collimator would have resolved this problem; however, risk of off-target toxicity to the spinal column and abdominal cavity would be introduced. As reported here, irradiating tumors between days 9 and 13 allowed for accurate application of fiducial clips and effective RT targeting, resulting in a physiologically relevant RT response.

Although SCRT reduces tumor burden in a subset of patients clinically, it is not 100% curative,[6] and we observed similar responses in our model, in which only a fraction of the irradiated tumors was controlled by therapy. This model will help us identify what factors dictate this divide and may therefore elucidate the mechanism behind this clinically relevant phenomenon. Additionally, there has been a recent paradigm shift in the field of radiation oncology toward coupling RT alongside other treatment modalities such as immunotherapy, chemotherapy, and dietary restrictions.[23,24] Having a well-established model for the investigation of such combinatorial approaches will be invaluable. For example, it will allow for the testing of various RT schedules, different doses, or alternative combinatorial therapies in an effort to devise an optimal strategy, or perhaps a novel treatment approach, that is both safe and therapeutically effective.

Conclusion

The innovative model presented here utilizes fiducial clips to demarcate tumor boundaries, allowing for precision targeting of SCRT to internal orthotopic rectal tumors. A clinically relevant SCRT regimen results in reduced tumor burden and enhanced overall survival. Additionally, clinically relevant RT-induced parameters such as increased fibrosis and HA production, alongside a reduction in tumor cellularity, are observed. Our technique is reproducible and recapitulates human RC, making it a useful model in further studying SCRT efficacy in RC.

Acknowledgments

The authors acknowledge Mary Georger from the Histology Core, Eric Hernady from the Small Animal Irradiation Core, and the Flow Cytometry Core at URMC for their help with this article.

Supplementary materials

Supplementary material associated with this article can be found in the online version at https://doi.org/10.1016/j.adro.2021.100867.

References

1. Bray F, Ferlay J, Soerjomataram I, Siegel RL, Torre LA, Jemal A. Global cancer statistics 2018: GLOBOCAN estimates of incidence and mortality worldwide for 36 cancers in 185 countries. *CA: Cancer J Clin*. 2018;68:394–424.
2. You YN, Habiba H, Chang GJ, Rodriguez-Bigas MA, Skibber JM. Prognostic value of quality of life and pain in patients with locally recurrent rectal cancer. *Ann Surg Oncol*. 2011;18:989–996.

3. Wilson TR, Alexander DJ. Clinical and non-clinical factors influencing postoperative health-related quality of life in patients with colorectal cancer. *Br J Surg*. 2008;95:1408–1415.
4. Pettersson D, Holm T, Iversen H, Blomqvist L, Glimelius B, Martling A. Preoperative short-course radiotherapy with delayed surgery in primary rectal cancer. *Br J Surg*. 2012;99:577–583.
5. Habr-Gama A, Sabbaga J, Gama-Rodrigues J, et al. Watch and wait approach following extended neoadjuvant chemoradiation for distal rectal cancer: Are we getting closer to anal cancer management? *Dis Colon Rectum*. 2013;56:1109–1117.
6. López-Campos F, Martín-Martín M, Fornell-Pérez R, et al. Watch and wait approach in rectal cancer: Current controversies and future directions. *World J Gastroenterol*. 2020;26:4218–4239.
7. Voskoglou-Nomikos T, Pater JL, Seymour L. Clinical predictive value of the in vitro cell line, human xenograft, and mouse allograft preclinical cancer models. *Clin Cancer Res*. 2003;9:4227–4239.
8. Gillespie MA, Steele CW, Lannagan TRM, Sansom OJ, Roxburgh CSD. Pre-clinical modelling of rectal cancer to develop novel radiotherapy-based treatment strategies. *Oncol Rev*. 2021;15:1–3.
9. Pahlman L. Improved survival with preoperative radiotherapy in resectable rectal cancer. *N Engl J Med*. 1997;23:62–627.
10. Kallman RF, Dorie MJ. Tumor oxygenation and reoxygenation during radiation therapy: Their importance in predicting tumor response. *Int J Rad Oncol Biol Phys*. 1986;12:681–685.
11. Lambregts DMJ, Maas M, Boellaard TN, et al. Long-term imaging characteristics of clinical complete responders during watch-and-wait for rectal cancer—an evaluation of over 1500 MRIs. *Eur Radiol*. 2020;30:272–280.
12. Dukes CE. The surgical pathology of rectal cancer. *J Clin Pathol*. 1949;2:95–98.
13. Orlando FA, Tan D, Baltodano JD, et al. *Standardized Pathology Report for Colorectal Cancer*. 2nd ed. Seoul, Korea: Gastrointestinal Pathology Study Group of the Korean Society of Pathologists; 2008.
14. Corbett TH, Griswold DP, Roberts BJ, Peckham JC, Schabel Jr. FM. Tumor induction relationships in development of transplantable cancers of the colon in mice for chemotherapy assays, with a note on carcinogen structure. *Cancer Res*. 1975;35:2434–2439.
15. van den Ende RPJ, Rigter LS, Kerkhof EM, et al. MRI visibility of gold fiducial markers for image-guided radiotherapy of rectal cancer. *Radiother Oncol*. 2019;132:93–99.
16. Hompes R, Cunningham C. Colorectal cancer: Management. *Medicine*. 2011;39:254–258.
17. Theodoropoulos GE, Lazaris AC, Theodoropoulos VE, et al. Hypoxia, angiogenesis and apoptosis markers in locally advanced rectal cancer. *Int J Colorectal Dis*. 2006;21:248–257.
18. Fang M, Yuan J, Peng C, Li Y. Collagen as a double-edged sword in tumor progression. *Tumour Biol*. 2014;35:2871–2882.
19. Znati CA, Rosenstein M, McKee TD, et al. Irradiation reduces interstitial fluid transport and increases the collagen content in tumors. *Clin Cancer Res*. 2003;9:5508–5513.
20. Straub JM, New J, Hamilton CD, Lominska C, Shnayder Y, Thomas SM. Radiation-induced fibrosis: Mechanisms and implications for therapy. *J Cancer Res Clin Oncol*. 2015;141:1985–1994.
21. Riehl TE, Foster L, Stenson WF. Hyaluronic acid is radioprotective in the intestine through a TLR4 and COX-2-mediated mechanism. *Am J Physiol Gastrointest Liver Physiol*. 2012;302:309–316.
22. de la Cruz-Merino L, Illescas-Vacas A, Grueso-López A, Barco-Sánchez A, Míguez-Sánchez C. Radiation for awakening the dormant immune system, a promising challenge to be explored. *Front Immunol*. 2014;5:102.
23. Roxburgh CS. Organ preservation in rectal cancer: Towards the norm rather than the exception. *Br J Surg*. 2021;108:745–747.
24. Klement RJ, Koebrunner PS, Meyer D, Kanzler S, Sweeney RA. Impact of a ketogenic diet intervention during radiotherapy on body composition: IV. Final results of the KETOCOMP study for rectal cancer patients. *Clin Nutr*. 2021;40:4674–4684.